JOURNAL OF AGRICULTURAL AND FOOD CHEMISTRY

Assessment of Anthocyanins in Grape (*Vitis vinifera* L.) Berries Using a Noninvasive Chlorophyll Fluorescence Method

GIOVANNI AGATI,*,† SYLVIE MEYER,§ PAOLO MATTEINI,† AND ZORAN G. CEROVIC§

Istituto di Fisica Applicata 'Nello Carrara', CNR, Via Madonna del Piano 10 (Edificio C), I-50019 Sesto Fiorentino, Italy, and Equipe de Biospectroscopie Végétale, Laboratoire d'Ecologie Systématique et Evolution, CNRS UMR 8079, Bât. 362, Université Paris-Sud, 91405 Orsay Cedex, France

Anthocyanins (Anths) in grape (*Vitis vinifera* L.) berries harvested at véraison from Pinot Noir and Pinot Meunier cultivars were assessed nondestructively by measuring chlorophyll fluorescence (ChlF) excitation spectra. With increasing Anth content, less excitation light was transmitted to the deeper Chl layers, and thus the ChlF signal decreased proportionally. By applying Beer−Lambert's law, the logarithm of the ratio between the fluorescence excitation spectra (log FER) from a green and a red berry gave the in vivo absorption spectrum of Anths, which peaked at about 540 nm. Absolute quantitative nondestructive determination of Anths for each berry was obtained by the log FER calculated for two excitation wavelengths, 540 and 635 nm (absorbed and not-absorbed by Anths, respectively) of ChlF at 685 nm. Over a range of skin colors going from green to purple, the relationship between the log [ChlF(635)/ChlF(540)] and the Anth concentration of berry extracts was fairly well fitted ($r^2 = 0.92$) using a power function. Reflectance spectra on the same berry samples were also measured, and Anth reflectance indices, which were originally developed for apples and table grapes, were derived. The log FER Anth index was superior to the reflectance-ratio-based index, but was as good as the color index for red grapes (CIRG) calculated from the whole visible reflectance spectrum. The proposed log FER method, applied by means of suitable portable devices, may represent a new, rapid, and noninvasive tool for the assessment of grape phenolic maturity in vineyards.

KEYWORDS: Anthocyanins; chlorophyll fluorescence; color index; grape berry; fluorescence excitation spectra; nondestructive determination; reflectance; ripening; *Vitis vinifera*

INTRODUCTION

Over the past two decades, big changes in the world's wine industry have occurred, mainly due to the augmented international competition from New World (North and South America, South Africa, and Australasia) wine producers (*1*). This phenomenon, along with the trend in consumer habits toward a reduced wine consumption, has led to an increased demand for high-quality wines (*1*, *2*). Consequently, the development and adaptation of new sophisticated and precise technologies to be used in viticulture are rapidly increasing (*3*).

Among the different aspects to be taken into account for premium wine production, an accurate assessment of grape maturity to determine the best harvest date is essential (*4*, *5*). Ripening of grape berries is a continuous process that passes through various stages (*6*); therefore, a precise date at which the fruit is universally considered to be mature is difficult to define. Several berry components for evaluating grape maturity have been suggested, such as sugar content, acidity, deformability and size, specific metabolites, visual color, and taste (*4*). A common practice consists of the periodic refractometrical measurement of the soluble solid (sugar) content of single berries, even if sugar accumulation is not well related to flavor and aroma compounds. Fruit tasting is also practiced; but this is a subjective judgment and requires an adequate sampling strategy (e.g., the samples tested must be representative of the entire harvested unit) (*7*).

More recently, the phenolic content of berries has been considered to be a fundamental parameter for wine quality, as it is responsible for the color, flavor, and structure of wine. Thus, the term "phenolic maturity" has been introduced (*8*, *9*). Phenolic compounds, and anthocyanins (Anths) in red grape varieties, are usually evaluated spectrophotometrically on solvent extracts of grape berries (*10*). The method is time-consuming and may produce certain artifacts due to pigment instability and loss of material. Also in this case, an accurate sampling approach that is representative of the vineyard under consideration is needed (*4*, *5*). Furthermore, the composition and evolution of berry phenolics with ripening depend on grape variety, viticultural practices, and environmental factors (*4*, *11*, *12*). Therefore, to

* Author to whom correspondence should be addressed (e-mail G.Agati@ifac.cnr.it; telephone +39 055 5225 306; fax +39 055 5225 305).
† Istituto di Fisica Applicata 'Nello Carrara'.
§ Université Paris-Sud.

10.1021/jf062956k CCC: $37.00
Published on Web 01/30/2007

determine the most appropriate time to harvest, a close monitoring of phenolics, starting from véraison, is usually performed (*4*, *8*).

Anthocyanins have been chosen as markers of phenolic maturation because of the simplicity and reliability of their dosage and because their evolution with ripening is equivalent to that of skin tannins (*13*, *14*). It has been shown that light intensity and nitrogen availability markedly affect the accumulation of different Anths in grape skin during ripening (*12*, *15*). The biosynthesis of Anths can be directly inhibited or enhanced by water deficit, depending on the period of occurrence and the severity of the stress (*16*). Dependence of Anth berry concentration on other factors, such as temperature (*17*), soil features (*18*), sunlight exposure (*19*), and defoliation practices (*20*), has also been reported. Because of this high variability, a rapid and nondestructive method to assess Anth content in situ would be of fundamental importance for vinegrowers.

For most red grape varieties, Anths are localized exclusively in the berry skin (*9*); therefore, their in situ detection can be performed using optical methods. Lamb et al. (*21*) proposed remote sensing multispectral imaging to predict grape color (Anth concentration) in a Cabernet Sauvignon vineyard by using the normalized difference vegetation index (NDVI). However, the correlation between Anths and NDVI was poor (maximal $r^2 = 0.33$) (*21*).

A color index for red grapes (CIRG) for an objective definition of the external color of red table grapes was introduced earlier (*22*). This index, based on colorimetric parameters, failed to accurately reproduce the evolution in Anths during ripening in a wine-making grape (Monastrell variety) (*23*). Reflectance diode array spectroscopy was tested to assess Anths in whole grape berries, obtaining a maximum of 0.50 for the coefficient of determination, in the correlation with the reference method, using the near-infrared (700−1100 nm) region (*24*). On the contrary, fairly good estimates of Anths in apple fruits, achieved by means of diffuse reflectance measurements, have been reported (*25*).

Recently, a new rapid and noninvasive fluorescence spectroscopic method for the in situ assessment of Anths in olive fruits has been developed (*26*) and extended to apples (*27*). It is based on a comparison of chlorophyll fluorescence (ChlF) signals at two different excitation wavelengths and is an extension of the techniques used to evaluate in situ the UV-absorbing phenolic compounds in leaf superficial layers (*28*−*30*). The method is based on the screening effect of compounds in the epidermal tissues, which decreases the excitation light available for ChlF. This recently developed approach can be named the ChlF screening method to distinguish it from the well-known ChlF practice used to evaluate the photosynthetic activity of plant material, which is the measurement of variable ChlF (Kautsky effect) (*31*).

In the present study, the ChlF screening method was applied to make a nondestructive assessment of the Anth content in grape berries with different skin colors, which correspond to different ripening levels. We were able to (i) measure the in vivo Anth absorption spectrum, (ii) calibrate the in vivo Anth absorbances with the Anth concentrations measured in methanol/water extracts from the same berry area used for the ChlF measurements, and (iii) determine the relative distribution of Anths and Chl in the berry skin in order to discuss the limit of the ChlF method. In addition, the ChlF screening method, reflectance indices, and CIRG were compared on the same berry samples in order to discuss the more efficient way to monitor the phenolic maturity in the vineyard.

MATERIALS AND METHODS

Samples and Procedures. Whole grape bunches of *Vitis vinifera* L., Pinot Noir and Pinot Meunier varieties, were harvested at véraison from an experimental vineyard in the Champagne region (Comité Interprofessionnel des Vins de Champagne, Épernay, France) on two sampling dates, namely, August 11 and 16, 2005. Berries with six different grades of color (green, green-pink, pink, red, violet, and dark violet) were collected and stored in 24-well polystyrene plates at 4 °C until used. Fluorescence and reflectance spectroscopies were performed on the apex of intact berries. After that, the berries were weighed, and their equatorial and meridian diameters were recorded using a caliper. Caps 7 mm in diameter were then cut from the berry apex with a razor blade, frozen in liquid nitrogen, and stored at −80 °C until Anth extraction was performed. Total soluble solids (sugars) in the juice from the remaining part of each berry was measured by means of refractometry (Refractometer Pocket PAL-1, Spectrum, Plainfield, IL) and expressed in degrees Brix. All measurements were carried out within 2 days from harvest. A total of 35 grape berries, 18 for Pinot Noir and 17 for Pinot Meunier, were analyzed.

Spectral Reflectance Measurements and Colorimetry. Total reflectance spectra from the berry apex were recorded in the 400−1000 nm range using a diode array spectrophotometer (HP8453, Agilent, Les Ulis, France) equipped with a Spectralon integrating sphere provided by Agilent (RSA accessory, Labsphere). Measurements were performed against Spectralon as a standard. The measured area had a diameter of 9 mm. Anth and Chl predicted concentrations were calculated from reflectance values at 550, 700, and 800 nm according to the method of Merzlyak et al. (*25*). The color of each berry was derived from the relative reflectance spectrum according to the convention of the CIELAB system (*32*). The lightness, reddish/greenish, and yellowish/bluish parameters, L^*, a^*, and b^*, respectively, were calculated by a suitable program using the D65 illuminant and a 10° standard observer. Derived parameters, such as hue angle ($h = \arctan b^*/a^*$) and chroma ($C^* = [(a^*)^2 + (b^*)^2]^{0.5}$), and the proposed (*22*) color index for red grapes [$\text{CIRG} = (180 - h)/(L^* + C^*)$] were then calculated. Negative h values derived from negative a^* numbers (green berries) were converted to angles in the 90−180° range.

Fluorescence Measurements and Elaboration. Excitation and emission fluorescence spectra of intact grape berries were acquired and corrected as described in a previous paper (*26*). The fluorescence signal was detected from the berry apex, through an optical fiber bundle at a 5-mm distance, integrating over a spot area of 6-mm diameter.

For each sample, excitation spectra were recorded in the 280−650 nm range for emission at 685 nm, whereas emission spectra were measured between 630 and 800 nm with the excitation at 436 nm.

As described before (*26*), the in vivo absorption spectrum of a berry, b_1, is given by

$$A_{b_1} = \log \frac{\text{ChlF}_{b_0}^{685}(\lambda_{ex})}{\text{ChlF}_{b_1}^{685}(\lambda_{ex})} \quad (1)$$

where b_0 represents a reference sample with zero absorbance in the spectral region of interest.

The ratio of ChlF at two excitation wavelengths is related to the ratio between the epidermal layer transmittances at the same wavelengths multiplied by a term that depends on the absorption properties of Chl (*29*). For emission at 685 nm, it is

$$\frac{\text{ChlF}^{685}(\lambda_1)}{\text{ChlF}^{685}(\lambda_2)} = \frac{T(\lambda_1)}{T(\lambda_2)} \times \left[\frac{\epsilon(\lambda_1)}{\epsilon(\lambda_1) + \epsilon(685)} \cdot \frac{\epsilon(\lambda_2) + \epsilon(685)}{\epsilon(\lambda_2)} \cdot \frac{1 - 10^{-[\epsilon(\lambda_1)+\epsilon(685)]C_{\text{Chl}}\ell}}{1 - 10^{-[\epsilon(\lambda_2)+\epsilon(685)]C_{\text{Chl}}\ell}}\right] \quad (2)$$

where ϵ and C_{Chl} are the molar absorptivity and concentration of Chl, respectively, and ℓ is the optical path length inside the sample.

The relationship between the FER at 685 nm and the Anth content can be found by choosing the excitation wavelength λ_1 inside the Anth absorption band and λ_2 (the reference) outside it, so that $T(\lambda_2) = 1$.

By applying the Beer−Lambert law ($A = \log T^{-1}$) and choosing 540 and 635 nm for λ_1 and λ_2, respectively, eq 2 becomes

$$\log \frac{\mathrm{ChlF}^{685}(635)}{\mathrm{ChlF}^{685}(540)} = A(540) + \log[\mathrm{DF}(C_{\mathrm{Chl}},685)] \qquad (3)$$

where

$$\mathrm{DF}(C_{\mathrm{Chl}},685) = \frac{\epsilon(635)}{\epsilon(635)+\epsilon(685)} \times \frac{\epsilon(540)+\epsilon(685)}{\epsilon(540)} \cdot \frac{1-10^{-[\epsilon(635)+\epsilon(685)]C_{\mathrm{Chl}}\ell}}{1-10^{-[\epsilon(540)+\epsilon(685)]C_{\mathrm{Chl}}\ell}} \qquad (4)$$

is defined as a distortion factor (DF). Equation 3 links the measured Chl FER directly to the Anth content, although the last term in it may introduce a distortion due to changes in the Chl concentrations during fruit ripening. Because the absorptivity coefficients of Chl at the two excitation wavelengths are nearly equal, the DF contribution is in any case minimized. In addition, the distortion effect due to Chl changes is not expected to be important in thick samples, such as fruits, in which the optical path length, ℓ, is large. According to eq 3, the in vivo quantitative assessment of Anths on intact berries was calculated by the log FER(635/540) and expressed as absorbance values. Reproducibility of the technique was checked by repeating measurement of the same berry side after repositioning and was found to be >98%.

Curve fitting was performed by means of Table Curve 2D software (v 3.04, Jandel Sci., San Rafael, CA), using the Simple Equations process.

Microscopy Analysis. Hand-cut cross sections (100−200 μm) of fresh berry skin mounted in water were immediately observed by the microscope system previously described (*33*) or under a Zeiss Axiophot microscope (Zeiss, Oberkohen, Germany) equipped with a color charge-coupled device (CCD) (Spot Insight QE, Diagnostic Instruments, Micromécanique, Évry, France) at the Cell Imaging Service (IBAIC, Université Paris-Sud, France). Absorbance spectra of Anth-containing hypodermal cells were obtained by measuring the light transmitted through the cross section using a ×40 objective lens and by comparing it to the light transmitted from a zone just outside the sample. Spectra of transmitted light were recorded by a CCD multichannel spectral analyzer (PMA 11-C5966, Hamamatsu, Photonics Italia, Arese, Italy) coupled to the microscope through an optical fiber bundle.

Multispectral imaging was performed by a monochrome CCD camera (Chroma CX260, DTA, Cascina, Italy) equipped with a motorized filter wheel carrying up to eight different interference filters. This detector made possible the sequential acquisition of transmittance and fluorescence images on specific spectral bands. Transmittance images for Anth localization were acquired at 546 nm (10-nm bandwidth, 546FS10-25, Andover Corp., Salem, NH). Fluorescence images of Chl and hydroxycinnamic acids were obtained by excitation at 365 nm (selected using a 10-nm bandwidth interference filter, 365FS10-25, Andover Corp.), with a dichroic mirror at 400 nm (ND400, Nikon) and detection filter at 680 nm (10-nm bandwidth, 680FS10-25, Andover Corp.) and 470 nm (10-nm bandwidth, 470FS10-25, Andover Corp.), respectively. Image spatial calibration using a ×10 Plan Fluor (NA = 0.3) objective was 0.79 μm/pixel. Image elaboration was performed using the Image-Pro Plus v 4.0 software (Media Cybernetics, Silver Spring, MD). Profiles of both fluorescence and transmittance signals from the cuticle into the berry mesocarp were obtained by plotting the mean intensity of each longitudinal row of pixels versus the depth.

Anthocyanin Extraction and Quantification. Freeze-dried berry caps were extracted using the Pirie and Mullins method (*13*). The advantage of this method is that, because it does not extract lipophilic compounds, chlorophylls and carotenoids, the extracts can be used directly for a spectroscopic estimation of phenolics. Dry samples were ground with three bursts of 20 s at maximal speed (30 Hz) (ball mill MM301, Retsch, Haan, Germany). The powder was transferred to 1 mL of acidified extraction solvent (50% MeOH, 0.1% HCl), vortexed for 30 s, and, after standing for 3 min, centrifuged for 3 min at 4100*g*. The pellet was re-extracted twice using the same procedure, and the final three pooled supernatants were adjusted precisely to 3 mL and then centrifuged again for 5 min at 4100*g*, for final clarification. The whole procedure was performed at room temperature (20−25 °C). Absorbance spectra were measured immediately upon extraction, from 200 to 1100 nm, on the spectrophotometer HP 8453 (Agilent, Les Ulis). Assessments of Anths from cap extracts were made according to the method of ref *15*. Anthocyanin contents were calculated on a skin surface basis. They were expressed in equivalents of malvidin 3-*O*-glucoside (oenin), the major Pinot Noir anthocyanin (*34*), using the molar absorptivity at 530 nm of 28500 M^{-1} cm^{-1} (28.5 μmol^{-1} cm^2) (corrected for often negligible residual absorbance at 780 nm). The absorptivity coefficient was obtained by measuring the standard malvidin 3-*O*-glucoside chloride (Extrasynthèse, Lyon, France) in the extraction solvent.

RESULTS AND DISCUSSION

Berry Tissue Localization of Anth and Chl. The use of Chl fluorescence excitation to detect compounds on vegetable surfaces requires a localization of the pigment-filtering layer above the Chl region. We therefore evaluated the distribution of Anth and Chl in the berry skin epidermal layers by means of transmittance and epifluorescence microscopy. The color transmission image of a red berry cross section reported in **Figure 1A** clearly shows the red layer of Anth-containing hypodermal cells located just below the epidermis. Besides the color, Anths are also evidenced by the absorption spectrum peaking at about 550 nm, which was measured in the red hypodermal cells by means of microspectrophotometry (**Figure 1B**), as well as by the image of absorbance at 546 nm represented in **Figure 2A**. Here, the signal from the cuticle and from cell walls of the inner tissue layers is an apparent absorbance due to scattering, rather than to pigment absorption. On the contrary, due to the vacuolar location of the pigment, the Anth layer appears as an almost homogeneous white stripe of authentic 546-nm absorbance. **Figure 2B** shows the merging of two fluorescence images sequentially acquired on the same red berry cross section of **Figure 2A**, recorded at 470 nm (light blue) and at 680 nm (red) under 365-nm excitation. Red and light blue fluorescence correspond to Chl and polyphenolics, respectively. The distribution of Chl is markedly inhomogeneous, due to the large morphological differences among cells of the skin layers and depending on the chloroplast subcellular location. The co-localization of Anths and Chl is well denoted by the intensity profiles reported in **Figure 2C**. Here, the absorbance at 546 nm (A_{546}) that is related to the Anth content and the ChlF (F_{680}) are plotted as a function of the depth along the direction indicated by the arrows in **Figure 2A**,**B**. The blue polyphenolic fluorescence shows well the berry cuticle. Our observation indicates that Anths are in the hypodermis cells and cover a layer with thickness of about 70 μm. Most of the Chl molecules are located 10−20 μm deeper than the first Anth layer; therefore, there is a significant, even if not complete, spatial separation between the two pigments. Accordingly, we can state that Anths in red grape berries are able to filter efficiently the light available to excite ChlF in the green spectral range, and, therefore, the usefulness of the log FER method for Anth assessment is assured.

In Vivo Anth Absorption Spectra from Chl Fluorescence Excitation Spectra. The excitation spectra of ChlF (at the 685-nm band) recorded on the surface of intact grape berries with different skin pigmentation are reported in **Figure 3A**, along with the emission spectrum of a green-red berry (b_3) excited at 436 nm. As expected, the excitation spectral shape is similar to the one previously observed in olive fruits (*26*), with maxima at about 440 and 480 nm, corresponding to the principal absorption peaks of chlorophylls *a* and *b* and carotenoids (cf.

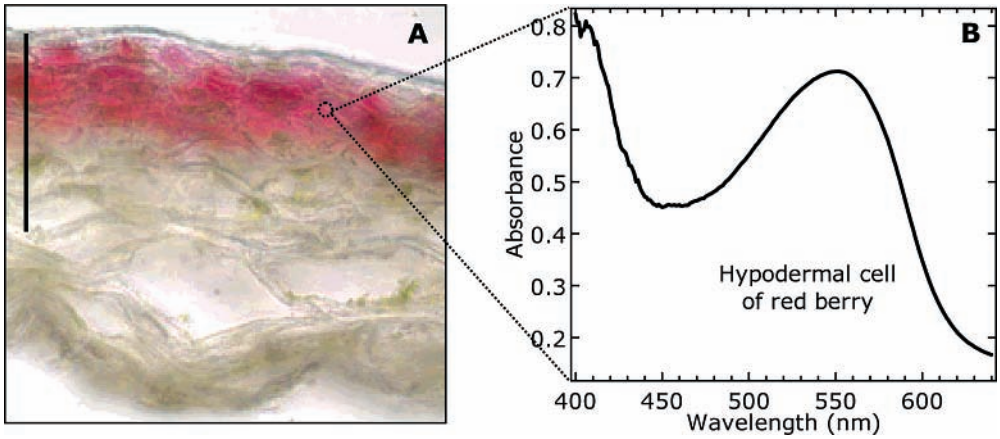

Figure 1. Color transmission image of a red berry (Pinot Noir) cross section, bar = 100 μm. (**A**) Absorbance spectrum of Anth-containing hypodermal cells obtained by measuring the light transmitted through the cross section using a ×40 objective lens and by comparing it to the light transmitted from a zone just outside the sample (**B**).

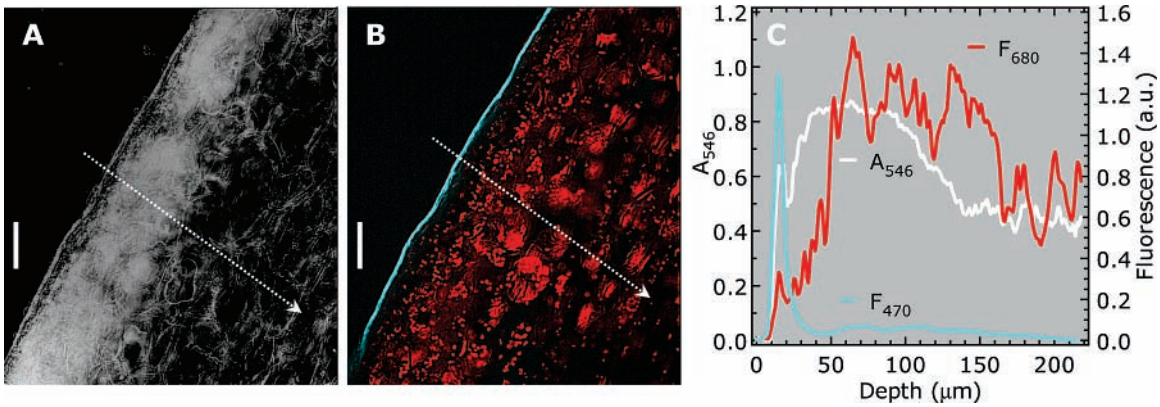

Figure 2. Microscopic analysis of a red berry cross section (Pinot Noir cultivar). (**A**) Absorbance image in the green spectral band of a red berry cross section calculated as $A = \log(1/T)$, where T is the section transmittance at 546 nm normalized to the one outside the sample; bar = 50 μm. (**B**) Recombination of two fluorescence images of the section in (**A**) recorded at 470 nm (light blue) and 680 nm (red) under 365 nm excitation. Red and light blue fluorescences correspond to Chl and hydroxycinnamic acids, respectively; bar = 50 μm. (**C**) Profiles of absorbance at 546 nm and fluorescence (F_{680} and F_{470}) from the cuticle into the berry mesocarp as the mean intensity of each longitudinal row of pixels versus the depth along the direction indicated by the arrows in (**A**) and (**B**).

ref *35*). A progressive reduction in ChlF intensity is observed with increasing redness (maturity) of the berry (from b_1 to b_6). Moreover, relatively larger reductions occur in the UV and green spectral regions due to the increasing superficial accumulation, with ripening, of flavonoids, hydroxycinnamates, and Anths, which filter the excitation light. In the difference absorption spectra among berries, calculated according to eq 1 as the logarithm of the Chl fluorescence excitation ratio (FER) of berries at increasing ripeness versus the greenest one (b_1) (**Figure 3B**), the absorption bands of Anths and flavonols, at about 540 and 380 nm, respectively, are markedly evident.

The Anth absorbance increases with increasing skin redness up to 1.36 units for b_6 with respect to b_1. Concurrently, absorbance at the flavonol band increases and shifts in wavelength from 360 to 390 nm moving from the b_1/b_2 to the b_1/b_6 FER. It is worth noting that the presence of adjacent absorption bands of hydroxycinnamic acids at about 300−320 nm and of Anths in the green (540 nm) can induce either a hypsochromic or a bathochromic apparent shift, respectively, in the maximum of flavonol absorption.

Further interesting aspects of the in vivo berry absorption properties can be deduced by comparing the log FER spectrum between a red berry (b_6 color level) and the same berry devoid of the skin (i.e., pulp) with the in vitro absorption spectrum of the methanolic extract of the very same skin (**Figure 3C**). The Anth bands in the two spectra are quite similar, whereas marked differences are observed in the UV range. In the in vitro spectrum, the flavonol peak is covered by larger absorbance at shorter wavelengths due to hydroxycinnamic acids present in the skin extract. On the other hand, the log FER spectrum possesses a valley at 330 nm that indicates the presence of larger quantities of hydroxycinnamic acids (mostly caffeic acid derivatives) in the pulp (*36*) with respect to the outer skin layers. These will screen pulp Chl and, therefore, decrease the log FER in which the pulp is used as reference (i.e., sample b_0 in eq 1).

The Anth band in vivo is quite similar to the band measured by means of microspectrophotometry on the hypodermal cells of a red berry (peak around 550 nm) (**Figure 2B**). It is shifted about 20 nm to longer wavelengths with respect to the absorbance spectra measured in vitro (peak at 528 nm in acidified methanol/water, 50:50 v/v).

At least three different causes could explain the position of the grape berry Anth maximum in vivo: (i) the contribution of different anthocyanins, (ii) the polarity of the environment, and (iii) the pH of the vacuole. Because the Anth compounds present in Pinot Noir grapes (delphinidin, cyanidin, petunidin, peonidin, and malvidin 3-glucosides) (*34*) have different absorption properties (*37*, *38*), the total Anth absorption spectrum will be the convolution of single compound spectra weighted according to the Anth concentrations. Malvidin 3-glucoside with in

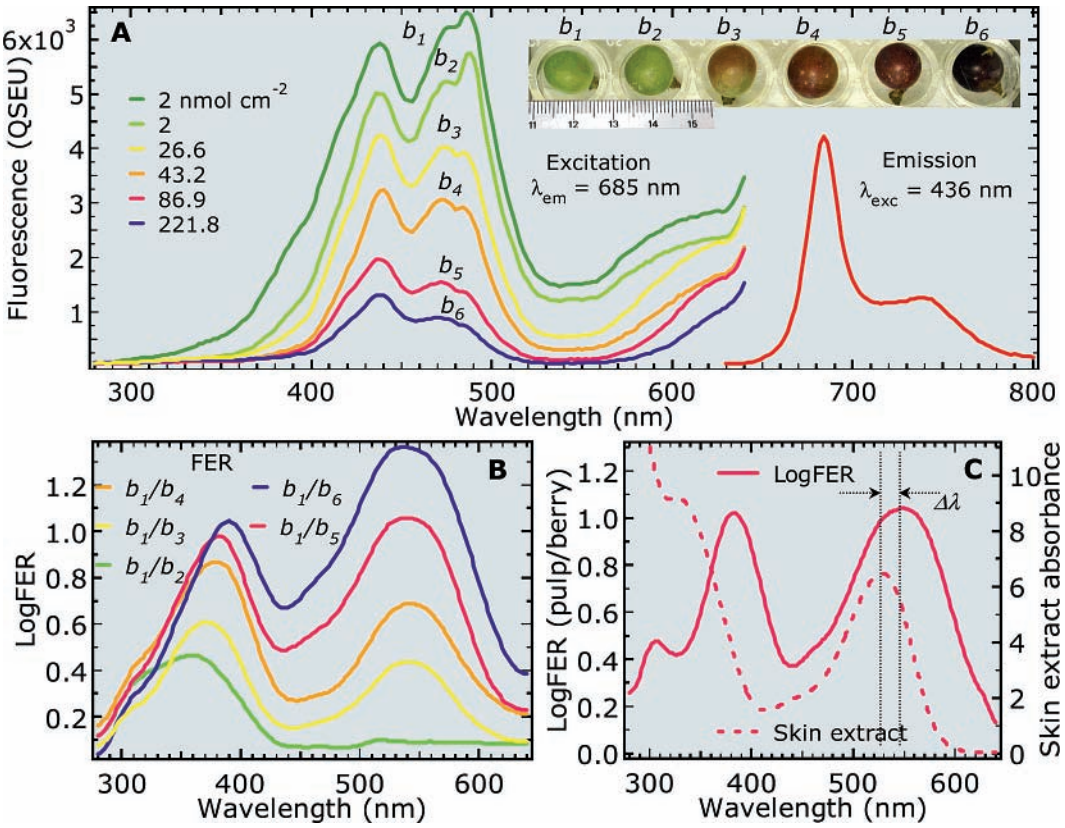

Figure 3. Fluorescence spectroscopy of grape berries. (**A**) ChlF excitation spectra obtained from the apex of intact berries with different skin colors (see inset); the emission wavelength was set at 685 nm; the emission spectrum of b_3 for excitation at 436 nm. (**B**) Difference absorbance spectra derived from the log FER of berries at increasing reddish color versus the greenest berry (b_1) for the Pinot Noir cultivar. (**C**) Absorbance spectrum derived from the log FER between a red berry and the same berry devoid of the skin and the respective in vitro absorption spectrum from the extracted anthocyanins.

vitro absorbance at the longest wavelengths (peak above 520 nm at pH 2−3) is the main contributor, as its relative concentration is up to 50% (*34*). Furthermore, the absorption maximum of Anths in solution is markedly dependent on the solvent (*37*). For example, the maximum of malvidin 3-glucoside is bathochromically shifted by 18 nm, going from water to methanol (at a constant pH). Finally, the peak wavelength of all Anth compounds is markedly dependent on pH, showing bathochromic shifts of up to 30−40 nm, ranging from 2.4 to 6.5 pH units (*38*), because of the change in proportion of the flavylium cation (red) to the quinoidal base form (blue) (*39*). Accordingly, the difference between the in vivo and in vitro Anth absorbance spectra may be explained by a higher vacuolar pH than the one used in vitro (pH 2.0). In particular, according to Cabrita et al. (*38*), the in vivo maximum recorded here at 548 nm would indicate a vacuolar pH for hypodermal cells of between 5 and 6.

A bathochromic shift induced by copigmentation (*40*) can probably be excluded for the following reasons. First, copigmentation due to both Anth self-association or Anth complexation to other compounds increases as a function of the Anth concentration (*41*). On the contrary, we did not observe any change in the absorbance peak wavelength with increasing Anth berry content, as shown by the absorbance spectra of **Figure 3B**. Second, no acylated Anths are present in Pinot Noir grapes (*34*), which indicates the absence of any intramolecular copigmentation in the grape berries.

A pH effect can also contribute to the large difference (6 times) between the absorbance values deduced by the log FER and those recorded in the skin extract (**Figure 3C**). According to the Henderson−Hasselbach equation calculated by Moskowitz and Hrazdina, with a pH of berry skin vacuoles of 2.7 (*42*) there will be 1.5 times less Anth in the flavylium cation (red colored) form than in the extract at pH 2. Alternatively, the inverse calculation that considers the observed absorbance ratio of 6 between in vitro and in vivo (**Figure 3C**) would result in a vacuolar pH of 3.39, which is still realistic.

Another contribution to this discrepancy between in vitro and in vivo absorbance is the inherent limitation of the log FER method due to the signal-to-noise ratio of the spectrofluorometer, as in any other technique based on measuring ratios. A ChlF of 1500 QSEU at 540 nm of the green berry, compared to 30 QSEU for a very red berry, yields a log FER of 1.7. However, the signal of the red berry represents only 2% of the green one, close to the stray light level in the front-face spectrofluorometer configuration. Therefore, the log FER cannot be expected to increase much further.

Log FER as in Vivo Signature of Anth Content. According to the log FER method, Chl acts as a natural photosensor that detects light transmitted through the most external layers of the berry skin and converts it into fluorescence. The photon−photon conversion performed by Chl molecules corresponds to the photon−electron conversion occurring in a standard spectrophotometer detector (photodiode or photomultiplier). Therefore, it is possible to measure Anth absorbance by comparing the ChlF signal excited with light that is particularly well absorbed and attenuated by Anth to the signal induced by light reaching Chl without attenuation. These values, which were calculated from the excitation spectra of each berry as log FER between 635 and 540 nm (eq 3), are plotted in **Figure 4** against the Anth concentration determined from the corresponding skin extract. Data from a total of 35 berries of the Pinot Noir and Pinot

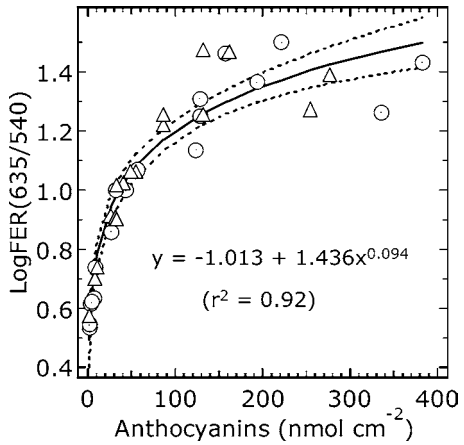

Figure 4. Relationship between Anth absorbance assessed nondestructively by the log FER at two excitation wavelengths, 635 and 540 nm, and the Anth concentration measured in the berry cap extracts from Pinot Noir (circles) and Pinot Meunier (triangles) grapes. Dotted lines indicate the 95% confidence limits.

Meunier cultivars with different skin color are reported. Their volume and total soluble sugars ranged from 0.67 to 1.57 cm^3 and from 5.5 to 18.0 °Brix, respectively, indicating different degrees of maturity.

The relationship between the log FER values and Anth concentration, expressed as oenin equivalents, was well fitted through a power function with a coefficient of determination, r^2, of 0.92 (fit standard error, $S_e = 0.087$). It is worth noting that the log FER value for green Anth-free berries is not nil. This is due to the contribution of the distortion factor defined in eq 4, induced by a slight difference in the molar absorptivities of Chls at the two excitation wavelengths (540 and 635 nm). The function of log FER against Anth content can be considered as linear for Anth concentrations up to about 90 nmol cm^{-2} ($r^2 = 0.91$, $S_e = 0.067$); thereafter, a saturation effect occurs. Possible causes for this result have been previously indicated for the analogous behavior observed in olive fruits (*26*). Accordingly, the main origin of the nonlinear behavior of the log FER versus Anth relationship reported in **Figure 4** seems to derive from the incomplete spatial separation between Anth and Chl layers (see **Figure 2**). With increasing berry ripeness, the Anth layer becomes thicker, the log FER method underestimates the Anth concentration and, consequently, a curvature in the log FER versus Anth graph reported in **Figure 4** is induced. Yet, an effect due to the presence of stray (unwanted) light in the spectrofluorometer, which is relatively more important when the signal-to-noise ratio is low (high Anth concentrations), contributes to limit the maximum measurable values of the log FER.

Comparison among Different Anth Optical Indices. Total reflectance spectra of representative berries at different Anth content are reported in **Figure 5A**. The minimum of reflectance in the red region at about 678 nm, corresponding to Chl absorption, did not change much with the Anth content. Also, below 500 nm, the reflectance was at low levels (between 4 and 7%), due to absorbance from Chl and carotenoids, and it remained almost unvaried with ripening. As expected, wide variability in reflectance among berries was recorded in the green spectral range as the result of an accumulation of Anths in the berry skin. The reflectance peak of green berries at 555 nm was reduced to a shoulder for Anths concentrations of just above 8 nmol/cm^2 and almost disappeared for Anths > 25 nmol/cm^2.

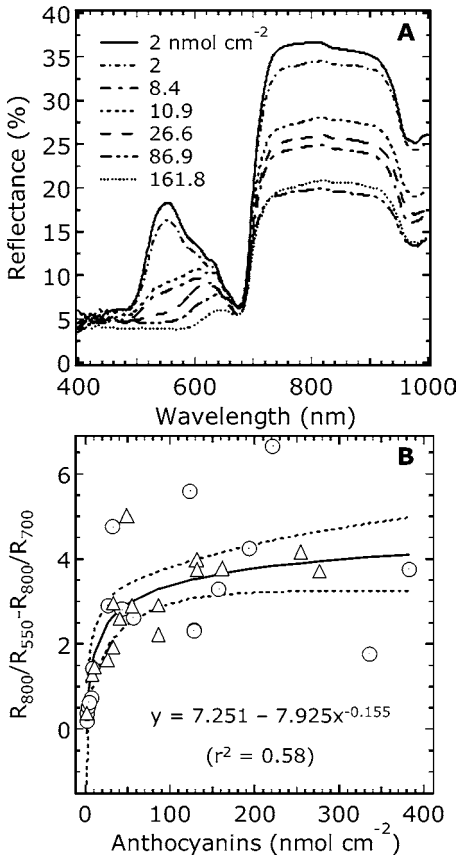

Figure 5. Reflectance spectroscopy of grape berries. (**A**) Total reflectance spectra from the apex of berries with different Anth contents. (**B**) Relationship between the Anth reflectance index $R_{800}(1/R_{550} - 1/R_{700})$ and the Anth concentration measured in the berry cap extracts from Pinot Noir (circles) and Meunier (triangles) grapes; dotted lines indicate the 95% confidence limits.

Considerable changes in reflectance were also observed in the NIR range: these might be due to structural changes occurring in the skin during maturation (*43*) and differences in berry sizes. From the above reflectance spectra, we estimated the berry Anth content using the R_{800} $(1/R_{550} - 1/R_{700})$ reflectance index recommended by Merzlyak et al. (*25*) for apple fruits. The resulting values were compared with the Anth concentrations of the corresponding skin extracts, as depicted in **Figure 5B**. The relationship obtained is similar to the log FER versus Anth one (power regression), but with a less accurate coefficient of determination ($r^2 = 0.58$, $S_e = 1.062$). Yet, even the fit of the same relationship at a low Anth content (up to 60 nmol/cm^2) was scarcely represented by a linear regression ($r^2 = 0.64$, $S_e = 0.842$). Other previously proposed Anth reflectance indices, where only $(R_{550})^{-1}$ and $(R_{700})^{-1}$ values are used without the NIR reflectance at 800 nm (*44*, *45*), provided an improved correlation with the actual Anth content ($r^2 = 0.68$, $S_e = 0.112$), but still far from the one obtained with the log FER index. It is worth noting that the Anth content of the apple skin was much smaller than for grape berries (even at this early stage of véraison). Merzlyak et al. (*25*) calibrated their index for the 2.5−50 nmol/cm^2 Anth range. The latter value corresponded to dark red apples and should be compared to 400 nmol/cm^2 found here in grape berries.

For each berry, the color index of red grapes (CIRG), as calculated from the hue angle (h), lightness (L^*), and chroma (C^*) coordinates of the CIELAB color space (*22*), was also compared to the Anth content (**Figure 6**). The CIRG increases

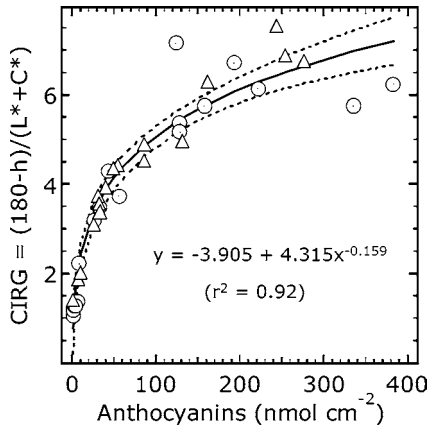

Figure 6. Relationship between the color index for red grapes [CIRG = (180 − *h*)/(*L** + *C**)] derived from the CIELAB *L**, *a**, and *b** parameters and the Anth concentration measured in the berry cap extracts from Pinot Noir (circles) and Pinot Meunier (triangles) grapes; dotted lines indicate the 95% confidence limits.

with increasing Anth accumulation, following a nonlinear relationship with a good correlation ($r^2 = 0.92$, $S_e = 0.557$). It is worth noting that all three colorimetric parameters used in the computation of CIRG (*h*, *C**, and *L**) showed a fine negative correlation with the Anth concentration (data not shown) and could be then used as maturation indices. However, the choice of the CIRG parameter makes it possible to define an index that increases as the berry color changes from green to dark violet.

In the computation of the colorimetric parameters, reflectance spectra are integrated over the visible spectral range once pondered by color-matching functions, in order to take into account the human eye's spectral response. Evidently, this processing, and the choice of an adequate color index (CIRG), match the berry Anth content better than the use of reflectance spectroscopy employing only three wavelengths.

The direct comparison between the log FER Anth index and the two colorimetric indices, which were originally developed for apples and table grapes, showed that log FER is superior to the reflectance-ratio-based index, but as good as the CIRG calculated from the whole visible reflectance spectrum. Nevertheless, the colorimetric index (CIRG) analyzed here was derived from total reflectance measured by an integrating sphere in contact with a single berry. It is not straightforward that the use of directional reflectance (at a distance) for a colorimetric analysis produces correlations with the Anth berry content that are as good as those obtained by using total reflectance. Therefore, in-field use of the colorimetric approach appears to be difficult and will require further experimental work.

For practical purposes, and when appropriate portable sensors become available, it would be interesting to compare the influence of the intensity, spectrum, and angle of incidence of the measuring light on CIRG versus log FER, in contact and from a distance. Natural light is known to have a great influence on both reflectance, such as the bidirectional and direct versus diffused light effects (*46*), and ChlF, such as the Kautsky induced effect (*31*).

As it is based on the ratio of fluorescence at two excitation wavelengths, the log FER method is independent of the shape and size of the samples. The log FER approach can also provide information on flavonols and hydroxycinnamic acids absorbing in the UV, whereas reflectance in this spectral range is very low and difficult to measure. Assessment of flavonols during ripening can represent an alternative maturation index in Anth-free white grape varieties.

According to our results, the proposed ChlF screening method, when applied by suitable portable devices, can represent a new rapid and noninvasive tool for the assessment of phenolic maturity in vineyards. Other ChlF-based techniques were applied in the past to the quality assessment of fruits (*47*), including grapes (*48*). Those approaches focused on the measurement of variable ChlF occurring at the dark-to-light transition (Kautsky effect) and then differ substantially from the present ChlF screening (log FER) technique. The log FER method does not require any dark adaptation of samples and so is suitable for a large number of sampling measurements, especially for in-field applications. For in-vineyard use, it is also important to note that dedicated portable fluorometers using the log FER method have already been applied to both apples in the laboratory (*27*) and leaves in in-field experiments (*49*).

The saturation effect in the calibration curve of log FER for skin Anth contents higher than 90 nmol/cm^2 may represent a limit in having a correct estimation of Anths at the late stages of grape maturity. However, the advantage of following a large number of samples during the ripening process permits one to carefully determine the function of Anth time evolution, which can be used as a parameter in harvest date decisions.

Future work will be devoted to finding the most appropriate ChlF excitation wavelengths and developing suitable optical devices to increase the signal-to-noise ratio at high Anth berry concentrations, for a further improvement of the technique.

ABBREVIATIONS USED

Anth(s), anthocyanin(s); Chl, chlorophyll; ChlF, chlorophyll fluorescence; CIRG, color index for red grapes; FER, fluorescence excitation ratio; log FER, logarithm of the fluorescence excitation ratio.

ACKNOWLEDGMENT

We thank Anne Aubusson Fleury (Service d'Imagerie Cellulaire, IBAIC, Faculté d'Orsay, France) for technical support and Alexandre Tonnellier and Laurent Panigai from CIVC for the supply of grapes and useful advice. G.A. is grateful to Bruno Radicati (IFAC-CNR) for the colorimetric analysis of berry reflectance spectra.

LITERATURE CITED

(1) Anderson, K.; Norman, D.; Wittwer, G. Globalization of the world's wine markets. *World Econ.* **2003**, *26*, 659−687.

(2) Bisson, L. F.; Waterhouse, A. L.; Ebeler, S. E.; Walker, M. A.; Lapsley, J. T. The present and future of the international wine industry. *Nature* **2002**, *418*, 696−699.

(3) Taylor, J.; Tisseyre, B.; Praat, J.-P. Bottling good information: mixing tradition and technology in vineyards. In *Information and Technology for Sustainable Fruit and Vegetable Production—FRUTIC 05 Symposium*, Sept 12−16, 2005, Montpellier France; Cemagref: Montpellier, pp 719−735.

(4) Krstic, M.; Moulds, G.; Panagiotopoulos, B.; West, S. *Growing Quality Grapes to Winery Specifications: Quality Measurement and Management Options for Grapegrowers*; Winetitles: Adelaide, Australia, 2003.

(5) Bramley, R. Understanding variability in winegrape production systems. 2. Within vineyard variation in quality over several vintages. *Aust. J. Grape Wine Res.* **2005**, *11*, 33−42.

(6) Coombe, B. G. Research on development and ripening of the grape berry. *Am. J. Enol. Vitic.* **1992**, *43*, 101−110.
(7) Winter, E.; Whiting, J.; Rousseau, J. *Winegrape Berry Sensory Assessment in Australia*; Winetitles: Adelaide, Australia, 2004.
(8) Institut Technique de la Vigne et du Vin. Journée technique régionale: Les composés phénoliques; 1998; http://www.itv-midipyrenees.com/publications/itv-colloque/colloque-composes-phenoliques.php.
(9) Kennedy, J. A.; Saucier, C.; Glories, Y. Grape and wine phenolics: history and perspective. *Am. J. Enol. Vitic.* **2006**, *57*, 239−248.
(10) Harbertson, J. F.; Spayd, S. Measuring phenolics in the winery. *Am. J. Enol. Vitic.* **2006**, *57*, 280−288.
(11) Mullins, M. G.; Bouquet, A.; Williams, L. E. *Biology of the Grapevine*; Cambridge University Press: Cambridge, U.K., 1992.
(12) Downey, M. O.; Dokoozlian, N. K.; Krstic, M. P. Cultural practice and environmental impacts on the flavonoid composition of grapes and wine: a review of recent research. *Am. J. Enol. Vitic.* **2006**, *57*, 257−268.
(13) Pirie, A. J. G.; Mullins, M. G. Interrelationships of sugars, anthocyanins, total phenols and dry weight in the skin of grape berries during ripening. *Am. J. Enol. Vitic.* **1977**, *28*, 204−209.
(14) de Montmollin, S.; Dupraz, P. Analyse de méthodes pour le suivi de la maturation phénolique des raisins de cépages rouges: essais préliminaires. *Rev. Suisse Vitic. Arboric. Hortic.* **2003**, *35*, 311−316.
(15) Keller, M.; Hrazdina, G. Interaction of nitrogen availability during bloom and light intensity during véraison. II. Effects on anthocyanin and phenolic development during grape ripening. *Am. J. Enol. Vitic.* **1998**, *49*, 341−349.
(16) Ojeda, H.; Andary, C.; Kraeva, E.; Carbonneau, A.; Deloire, A. Influence of pre- and postvéraison water deficit on synthesis and concentration of skin phenolic compounds during berry growth of *Vitis vinifera* L. cv. Shiraz. *Am. J. Enol. Vitic.* **2002**, *53*, 261−267.
(17) Yamane, T.; Jeong, S. T.; Goto-Yamamoto, N.; Koshita, Y.; Kobayashi, S. Effects of temperature on anthocyanin biosynthesis in grape berry skins. *Am. J. Enol. Vitic.* **2006**, *57*, 54−59.
(18) Yokotsuka, K.; Nagao, A.; Nakazawa, K.; Sato, M. Changes in anthocyanins in berry skins of Merlot and Cabernet Sauvignon grapes grown in two soils modified with limestone or oyster shell versus a native soil over two years. *Am. J. Enol. Vitic.* **1999**, *50*, 1−12.
(19) Bergqvist, J.; Dokoozlian, N.; Ebisuda, N. Sunlight exposure and temperature effects on berry growth and composition of Cabernet sauvignon and Grenache in the central San Joaquin valley of California. *Am. J. Enol. Vitic.* **2001**, *52*, 1−7.
(20) Hunter, J. J.; De Villiers, O. T.; Watts, J. E. The effect of partial defoliation on quality characteristics of *Vitis vinifera* L. cv. Cabernet Sauvignon grapes. II. Skin color, skin sugar, and wine quality. *Am. J. Enol. Vitic.* **1991**, *42*, 13−18.
(21) Lamb, D. W.; Weedon, M. M.; Bramley, R. G. V. Using remote sensing to predict grape phenolics and colour at harvest in a Cabernet Sauvignon vineyard: timing observations against vine phenology and optimising image resolution. *Aust. J. Grape Wine Res.* **2004**, *10*, 46−54.
(22) Carreño, J.; Martínez, A.; Almela, L.; Fernández-López, J. A. Proposal of an index for the objective evaluation of the colour of red table grapes. *Food Res. Int.* **1995**, *28*, 373−377.
(23) Fernández-López, J. A.; Almela, L.; Muñoz, J. A.; Hidalgo, V.; Carreño, J. Dependence between colour and individual anthocyanin content in ripening grapes. *Food Res. Int.* **1998**, *31*, 667−672.
(24) Cozzolino, D.; Esler, M. B.; Dambergs, R. G.; Cynkar, W. U.; Boehm, D. R.; Francis, I. L.; Gishen, M. Prediction of colour and pH in grapes using a diode array spectrophotometer (400−1100 nm). *J. Near Infrared Spectrosc.* **2004**, *12*, 105−111.
(25) Merzlyak, M. N.; Solovchenko, A. E.; Gitelson, A. A. Reflectance spectral features and non-destructive estimation of chlorophyll, carotenoid and anthocyanin content in apple fruit. *Postharvest Biol. Technol.* **2003**, *27*, 197−211.
(26) Agati, G.; Pinelli, P.; Cortes-Ebner, S.; Romani, A.; Cartelat, A.; Cerovic, Z. G. Nondestructive evaluation of anthocyanins in olive (*Olea europaea*) fruits by in situ chlorophyll fluorescence spectroscopy. *J. Agric. Food Chem.* **2005**, *53*, 1354−1363.
(27) Hagen, S. F.; Solhaug, K. A.; Bengtsson, G. B.; Borge, G. I. A.; Bilger, W. Chlorophyll fluorescence as a tool for non-destructive estimation of anthocyanins and total flavonoids in apples. *Postharvest Biol. Technol.* **2006**, *41*, 156−163.
(28) Bilger, W.; Veit, M.; Schreiber, L.; Schreiber, U. Measurement of leaf epidermal transmittance of UV radiation by chlorophyll fluorescence. *Physiol. Plant.* **1997**, *101*, 754−763.
(29) Ounis, A.; Cerovic, Z. G.; Moya, I.; Briantais, J. M. Dual-excitation FLIDAR for the estimation of epidermal UV absorption in leaves and canopies. *Remote Sens. Environ.* **2001**, *76*, 33−48.
(30) Cerovic, Z. G.; Ounis, A.; Cartelat, A.; Latouche, G.; Goulas, Y.; Meyer, S.; Moya, I. The use of chlorophyll fluorescence excitation spectra for the non-destructive in situ assessment of UV-absorbing compounds in leaves. *Plant Cell Environ.* **2002**, *25*, 1663−1676.
(31) Papageorgiou, G. C.; Govindjee. Chlorophyll *a* fluorescence. A signature of photosynthesis. In *Advances in Photosynthesis and Respiration*; Govindgee, Ed.; Springer: Dordrecht, The Netherlands, 2004.
(32) Wyszecki, G.; Stiles, W. S. *Color Science*; Wiley: New York, 1982.
(33) Agati, G.; Galardi, C.; Gravano, E.; Romani, A.; Tattini, M. Flavonoid distribution in tissues of *Phillyrea latifolia* L. leaves as estimated by microspectrofluorometry and multispectral fluorescence microimaging. *Photochem. Photobiol.* **2002**, *76*, 350−360.
(34) Mazza, G.; Fukumoto, L.; Delaquis, P.; Girard, B.; Ewert, B. Anthocyanins, phenolics, and color of Cabernet Franc, Merlot, and Pinot Noir wines from British Columbia. *J. Agric. Food Chem.* **1999**, *47*, 4009−4017.
(35) Louis, J.; Cerovic, Z. G.; Moya, I. Quantitative study of fluorescence excitation and emission spectra of bean leaves. *J. Photochem. Photobiol. B: Biol.* **2006**, *85*, 65−71.
(36) Adams, D. O. Phenolics and ripening in grape berries. *Am. J. Enol. Vitic.* **2006**, *57*, 249−256.
(37) Hebrero, E.; Santos-Buelga, C.; Rivas-Gonzalo, J. C. High performance liquid chromatography−diode array spectroscopy identification of anthocyanins of *Vitis vinifera* variety Tempranillo. *Am. J. Enol. Vitic.* **1988**, *39*, 227−233.
(38) Cabrita, L.; Fossen, T.; Andersen, Ø. M. Colour and stability of the six common anthocyanidin 3-glucosides in aqueous solutions. *Food Chem.* **2000**, *68*, 101−107.
(39) Cheynier, V.; Duenas-Paton, M.; Salas, E.; Maury, C.; Souquet, J.-M.; Sarni-Manchado, P.; Fulcrand, H. Structure and properties of wine pigments and tannins. *Am. J. Enol. Vitic.* **2006**, *57*, 298−305.
(40) Boulton, R. The copigmentation of anthocyanins and its role in the color of red wine: a critical review. *Am. J. Enol. Vitic.* **2001**, *52*, 67−87.
(41) Mazza, G.; Brouillard, R. The mechanism of co-pigmentation of anthocyanins in aqueous solutions. *Phytochemistry* **1990**, *29*, 1097−1102.
(42) Moskowitz, A. H.; Hrazdina, G. Vacuolar contents of fruit subepidermal cells from *Vitis* species. *Plant Physiol.* **1981**, *68*, 686−692.
(43) Considine, J. A.; Knox, R. B. Development and histochemistry of the cells, cell walls, and cuticle of the dermal system of fruit of the grape, *Vitis vinifera* L. *Protoplasma* **1979**, *99*, 347−365.
(44) Merzlyak, M. N.; Chivkunova, O. B. Light-stress-induced pigment changes and evidence for anthocyanin photoprotecion

in apples. *J. Photochem. Photobiol. B: Biol.* **2000**, *55*, 155−163.
(45) Gitelson, A. A.; Merzlyak, M. N.; Chivkunova, O. B. Optical properties and nondestructive estimation of anthocyanin content in plant leaves. *Photochem. Photobiol.* **2001**, *74*, 38−45.
(46) Govaerts, M.; Jacquemoud, S.; Verstraete, M. M.; Ustin, S. L. Three-dimensional radiation transfer modeling in a dicotyledon leaf. *Appl. Opt.* **1996**, *35*, 6585−6598.
(47) DeEll, J. R.; van Kooten, O.; Prange, R. K.; Murr, D. P. Applications of chlorophyll fluorescence techniques in postharvest physiology. *Hortic. Rev.* **1999**, *23*, 69−107.
(48) Kolb, C. A.; Wirth, E.; Kaiser, W. M.; Meister, A.; Reiderer, M.; Pfündel, E. E. Noninvasive evaluation of the degree of ripeness in grape berries (*Vitis vinifera* L. Cv. Bacchus and Silvaner) by chlorophyll fluorescence. *J. Agric. Food Chem.* **2006**, *54*, 299−305.
(49) Cartelat, A.; Cerovic, Z. G.; Goulas, Y.; Meyer, S.; Lelarge, C.; Prioul, J.-L.; Barbottin, A.; Jeuffroy, M.-H.; Gate, P.; Agati, G.; Moya, I. Optically assessed contents of leaf polyphenolics and chlorophyll as indicators of nitrogen deficiency in wheat (*Triticum aestivum* L.). *Field Crops Res.* **2005**, *91*, 35−49.

Received for review October 13, 2006. Revised manuscript received December 11, 2006. Accepted December 11, 2006. This work was supported by the CNR (Italy)−CNRS (France) bilateral co-operation project 16256.

JF062956K